Supplementary Information
for
New Magnetic Frameworks of [$(CuF_2(H_2O)_2)_x$(pyz)]

A. Lanza,[ab] *C. Fiolka,*[a] *M. Fisch,*[ab] *N. Casati,*[b] *M. Skoulatos,*[c] *C. Rüegg,*[cd] *K. W. Krämer*[a] *and Piero Macchi*[*a]

[a] Department of Chemistry and Biochemistry, University of Bern, Freiestrasse 3, 3012 Bern, Switzerland.

[b] Swiss Light Source, Paul Scherrer Institute, CH-5232 Villigen, Switzerland.

[c] Laboratory for Neutron Scattering and Imaging, Paul Scherrer Institute, CH-5232 Villigen, Switzerland.

[d] DPMC-MaNEP, University of Geneva, CH-1211 Geneva, Switzerland.

Contents:

Crystallization of [($CuF_2((H/D)_2O)_2)_x$(pyz)] species

Copper(II) chloride (12.907 g, 96 mmol) was dissolved in 192 ml water and a solution of silver nitrate (32.616 g, 192 mmol) in 96 ml water was added. The mixture was stirred and the precipitate was filtered off. The filtrate was cooled to 5 °C. Ammonium fluoride (7.112 g, 192 mmol) and pyrazine (7.689 g, 96 mmol) in 96 ml water was added at 5 °C and the final solution was divided into 4 – 6 parts and poured into beakers. The solvent was slowly evaporated at 5 °C. Typically crystals up to one gram of compound **1** were obtained. Elemental analysis was performed with a Thermo Scientific Flash 2000 Organic Elemental Analyzer for [$CuF_2(H_2O)_2$(pyz)] (**1**): calcd C 22.07, H 3.70, N 12.87, O 14.70; found C 22.01, H 3.77, N 12.74, O 15.16 %. After a long period of evaporation of the mother liquor, compound **2** crystallizes from the solution and in some cases it grows epitactic on the 100 face of compound **1**. **2** can undergo decomposition at room temperature, especially in powder form. Samples of **2** were stored either in the mother liquor or at –80 °C. Elemental analysis of [($CuF_2(H_2O)_2)_2$(pyz)] (**2**): calcd C 13.52, H 3.40, N 7.89, O 18.02; found C 13.57, H 3.47, N 7.80, O 18.82 %.

With the same procedure and using deuterated reagents and solvents crystals of the perdeuterated species [($CuF_2(D_2O)_2)_x$(pyz)] could be obtained with the same yield and quality. For most experiments we used deuterated crystals.

Characterization of [$CuF_2(D_2O)_2$(pyz)] (1)

HP SC-XRD and crystal structure of ε–[$CuF_2(D_2O)_2$(pyz)]

A crystal of [$CuF_2(D_2O)_2$(d_4-pyz)] (ca. 0.15×0.10×0.05 mm^3) was loaded in a Merrill-Bassett diamond-anvil cell equipped with 0.5 mm diamonds and a steel gasket, pre-indented to 0.080 mm and with a 0.20 mm hole diameter. Isopropanol was used as pressure transmitting medium (PTM) and pressure was calibrated with the ruby fluorescence method.[13] The diffracted intensities were collected at 3.3 GPa and R.T. with an Oxford Diffraction SuperNova area-detector diffractometer using mirror optics monochromated Mo *K*α radiation (λ = 0.71073 Å). A total of 752 frames were collected in 1° ω steps, 30 or 50 seconds as theta-dependent exposure time and a fixed sample-detector distance of 68.0 mm; CrysAlisPro[14] was used for the data collection, data reduction and empirical absorption correction. The crystal structure for phase **ε–1** was solved by direct methods with SHELXS-2013[15] and least-squares refined with SHELXL-2013[15] using isotropic thermal parameters for all atoms. D atoms for the pyrazine ring were assigned geometrically and refined with a riding model with isotropic thermal parameter (U_{iso}) equal to 1.2 times that of the corresponding parent atom. D atoms pertaining to the coordinated water molecule were located in the Fourier difference map and refined with a restrained O–D distance.

The results of this experiment are reported in Tables S1 and S2. With the same setup we measured two further pressure points at 3.6 and 4.3 GPa, which showed no further phase transition. The data quality is decreasing with increasing pressure so the structure is not worth being discussed further. The experiment was repeated once again with a deuterated sample and once with a hydrogenated sample. In both cases the crystals broke and so no decent data could be obtained for structure determination, but the multicrystal indexing performed with CrysAlisPro[14] confirmed again the presence of phase **ε–1**. The non-conventional crystallographic setting *A*–1 was chosen to allow straightforward comparison of **ε–1** with the other crystal structures of **1**. This centered unit cell can be obtained from the primitive one (standard setting *P*–1) by applying the transformation matrix: $\begin{pmatrix} -1 & 0 & -1 \\ 1 & 1 & 0 \\ 1 & -1 & 0 \end{pmatrix}$ and a $(0\ 0.5\ 0.5)$ translation.

Table S1. Crystal data and structure refinement for **ε-1** at 3.3 GPa.

ε-$CuF_2(H_2O)_2$(pyz)	CCDC 998110	
Empirical formula, M_r	$C_4 D_8 Cu F_2 N_2 O_2$	225.71 g mol^{-1}
T, *P*	297.5(4) K,	3.3 GPa
λ	0.71073 Å	
Crystal system	Triclinic	
Space group, *Z*	*A*-1,	2
Unit cell dimensions	a = 6.813(4) Å	α= 84.344(15) °
	b = 7.1823(11) Å	β= 116.72(4) °
	c = 7.4463(12) Å	γ = 78.85(3) °
Volume	312.1(2) $Å^3$	
Unit cell dimensions in standard setting, P-1	*a = 4.9115(9) Å*	*α= 99.8(3) °*
	b = 5.4216(9) Å	*β= 105.24(4)°*
	c = 6.187(4) Å	*γ = 92.078(13) °*
Volume in P-1	*156.05(12) $Å^3$*	
Z in P-1	*1*	
Crystal dimensions	0.15 × 0.1 × 0.5 mm^3	
Density (calculated), μ	2.402 Mg m^{-3},	3.485 mm^{-1}
F(000)	218	
θ range	3.828 to 27.357 °	
Index ranges	-5<=h<=5, -8<=k<=8, -9<=l<=9	
Reflections (unique), R_{int}	831 (182),	0.0675
Parameters (restraints)	28 (1)	
Goodness-of-fit on F^2	1.100	
R indices [I>2σ(I)]	R_1 = 0.0556,	wR_2 = 0.1429
R indices (all data)	R_1 = 0.0568,	wR_2 = 0.1440
Largest diff. peak and hole	0.769 and -0.900 e.$Å^{-3}$	

Table S2. Selected geometric parameters and H-bond details for **ε-1**

atoms[a]	*distance* /Å	*atoms*	*distance* /Å
Cu1—F1	1.886(5)	Cu1—O1	2.360(12)
Cu1—N1	2.00(2)		
atoms	*angle* /°	*atoms*	*angle* /°
F1—Cu1—F1$^{\mathrm{i}}$	180.0	N1—Cu1—O1	92.8(7)
F1—Cu1—N1	91.6(5)	N1—Cu1—O1$^{\mathrm{i}}$	87.2(7)
F1$^{\mathrm{i}}$—Cu1—N1	88.4(5)	N1—Cu1—N1$^{\mathrm{i}}$	180.0
F1—Cu1—O1$^{\mathrm{i}}$	94.8(3)	O1$^{\mathrm{i}}$—Cu1—O1	180.0
F1—Cu1—O1	85.2(3)		

X—D···*A*[a]	*X*···*A* /Å	*X*—D···*A* /°[b]
O1—D1*A*···F1$^{\mathrm{ii}}$	2.692(15)	148(24)
O1—D1*B*···F1$^{\mathrm{iii}}$	2.655(18)	154(14)
C1—D1···O1$^{\mathrm{i}}$	3.02(2)	121
C2—D2···O1	3.15(4)	115
C2—D2···F1$^{\mathrm{ii}}$	3.20(3)	175

[a] Symmetry codes: (i) -*x*, -*y*, -*z*; (ii) -*x*, -*y*-1/2, -*z*-1/2; (iii) *x*, *y*+1/2, *z*-1/2. [b] The uncertainty is not given in case the D coordinates are not freely refined.

Table S3. Lattice parameters for **ε-1** from SC-XRD as a function of P.

Phase name	**ε-1**		
Crystal system	Triclinic		
Space group, *Z*	*A*-1, *2*		
P (GPa)	3.3	3.5	4.4
Unit cell dimensions:			
a /Å	6.813(4)	6.7933(17)	6.768(2)
b /Å	7.1823(11)	7.1580(4)	7.1063(5)
c /Å	7.4463(12)	7.4280(4)	7.3885(5)
α /°	84.344(15)	84.331(5)	84.298(6)
β /°	116.72(4)	116.805(12)	117.022(14)
γ /°	78.85(3)	78.589(11)	77.999(14)
V /Å^3	312.1(2)	308.63(9)	301.88(10)

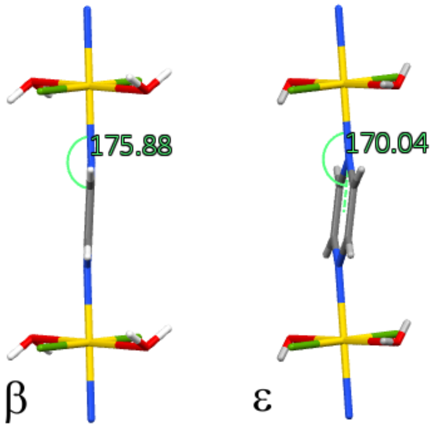

Figure S1 – Side view of the polymeric chains of **1**, showing the tilting angle of pyrazine rings with respect to the Cu-Cu direction.

HP P-XRD

The P-XRD experiments were performed at the X04SA Material Science Beamline at the Swiss Light Source, Paul Scherrer Institut, Villigen, Switzerland.[16] The beamline is equipped with a Mythen II microstrip detector and the beam was focussed and monochromatized to 16 keV (a silicon standard was used for fine calibration of the energy). Single crystals of $CuF_2(D_2O)_2(d_4\text{-pyz})$ were ground and loaded in a membrane-driven diamond anvil cell (DAC) equipped with 0.5 mm diamond anvils and steel gaskets, with typical thickness 0.070-0.090 mm and hole diameter 0.200 mm. The pressure was calibrated either with the ruby fluorescence method[13] or from the equation of state of quartz added as internal standard.[17] 5 groups of experiments were performed, which differed for the pressure increase rate applied or for the PTM according to Table S4.

Table S4. Summary of the P-XRD experimental conditions.

Experiment	*PTM*	*Pressure increase rate*
1	isopropanol	Medium (ca. 0.5 GPa/h)
2	isopropanol	High (ca. 15 GPa/h)
3	isopropanol	Low (ca. 0.1 GPa/h)
4	petrol ether	not constant
5	fluorinert	not constant

From every experiment, the lattice parameters for every present phase were refined with Topas Academic[18] Figure 2 (in the main text) was obtained from all the experimental points listed in Table S5, which are coming from different experiments.

Table S5. Lattice parameters for **1** refined from P-XRD experiments.

	Experiment	**P / GPa**	**a / Å**	**b / Å**	**c / Å**	**β / °**	**V / Å^{3}**
Phase α-1	1	0.00(9)	7.6893(2)	7.56545(14)	6.9001(3)	111.205(5)	374.22(3)
	2	0.05(9)	7.6800(2)	7.5619(2)	6.8932(3)	111.314(4)	372.95(3)
	2	0.10(9)	7.66993(14)	7.55619(17)	6.8839(2)	111.557(3)	371.052(17)
	1	0.21(9)	7.6626(4)	7.54558(9)	6.8634(5)	111.885(8)	368.23(4)
	4	0.31(9)	7.63606(14)	7.54001(10)	6.8595(16)	112.095(2)	365.939(13)
	2	0.48(9)	7.6200(3)	7.5181(3)	6.8213(4)	112.747(5)	360.39(3)
	1	0.71(9)	7.6064(3)	7.49598(6)	6.7884(3)	113.318(6)	355.44(3)
	4	0.93(9)	7.5854(14)	7.4776(6)	6.7798(12)	113.839(15)	351.75(10)
	5	1.44(9)	7.5259(12)	7.5109(10)	6.7009(15)	114.540(18)	344.56(12)

	Experiment	**P / GPa**	**a / Å**	**b / Å**	**c / Å**	**β / °**	**V / Å^{3}**
Phase β-1	1 (decomp)	0.63(9)	6.8909(5)	7.7201(15)	7.1793(6)	113.229(9)	350.97(5)
	2	0.97(9)	6.8778(5)	7.68937(14)	7.1249(6)	113.906(9)	344.48(4)
	1	1.11(9)	6.8703(4)	7.67576(12)	7.1103(5)	114.108(7)	342.25(3)
	5	1.44(9)	6.86490(15)	7.63330(18)	7.0799(2)	114.470(3)	337.676(18)
	2	1.65(9)	6.8501(3)	7.6193(2)	7.0479(3)	114.863(4)	333.75(2)
	4	1.85(9)	6.84848(11)	7.5741(3)	7.0591(3)	115.180(2)	331.37(2)
	1	1.93(9)	6.8385(4)	7.5902(2)	7.0305(5)	115.253(6)	330.04(3)
	3	2.00(9)	6.8320(3)	7.5729(3)	7.0195(4)	115.430(6)	327.98(3)
	3	2.17(9)	6.82668(18)	7.55229(15)	7.0086(2)	115.631(3)	325.790(17
	2	2.37(9)	6.8209(3)	7.5340(3)	7.0023(4)	115.754(5)	324.10(3)
	4	2.52(9)	6.8282(2)	7.4995(5)	6.9856(4)	115.916(4)	321.75(3)
	1	2.80(9)	6.80906(18)	7.48622(19)	6.9850(2)	116.165(3)	319.566(17)
	2	3.15(9)	6.7980(3)	7.4349(7)	6.9812(4)	116.565(6)	315.60(3)
	1	3.53(9)	6.7901(3)	7.3864(2)	6.9576(3)	116.514(5)	312.25(2)
	2	3.81(9)	6.788(3)	7.3691(6)	6.950(4)	116.97(5)	309.8(3)

	Experiment	**P / GPa**	**a / Å**	**b / Å**	**c / Å**	**β / °**	**V / Å^{3}**
Phase γ-1	3	3.20(9)	6.8464(13)	7.7223(11)	6.5696(16)	117.38(2)	308.43(12)
	3	3.40(9)	6.8294(3)	7.7029(2)	6.5577(3)	117.147(5)	306.97(3)
	1	3.53(9)	6.8280(10)	7.6994(8)	6.5725(10)	117.428(16)	306.69(8)
	2	3.81(9)	6.8191(8)	7.6673(7)	6.5688(10)	117.537(14)	304.54(7)
	1 (decomp)	3.83(9)	6.8181(10)	7.6697(9)	6.5484(12)	117.364(18)	304.12(9)
	1	3.84(9)	6.8177(5)	7.6677(4)	6.5503(6)	117.385(9)	304.05(5)
	3	4.10(9)	6.8121(15)	7.6394(11)	6.5445(15)	117.61(2)	301.80(12)
	1	4.18(9)	6.8105(13)	7.6374(12)	6.5436(16)	117.56(2)	301.73(12)
	2	4.35(9)	6.8071(7)	7.6039(7)	6.5684(9)	117.914(13)	300.43(7)
	3	4.58(9)	6.8055(4)	7.6197(3)	6.5417(5)	117.762(7)	300.17(4)
	2	4.91(9)	6.8104(14)	7.5371(12)	6.5520(17)	118.09(2)	296.71(13)

	Experiment	**P / GPa**	**a / Å**	**b / Å**	**c / Å**	**α / °**	**β / °**	**γ / °**	**V / Å^{3}**	**2V / Å^{3}**
Phase ε-1 (in P-1!)	1 (decomp)	3.83(9)	4.8852(10)	5.3861(9)	6.0866(12)	99.94(2)	104.181(14)	92.435(17)	152.34(5)	304.68(7)
	3	4.10(9)	4.8563(18)	5.3731(17)	6.088(2)	100.07(4)	104.52(3)	92.24(3)	150.85(10)	301.70(14)
	1	4.18(9)	4.8701(13)	5.3727(11)	6.0591(14)	99.90(2)	103.997(18)	92.02(2)	151.05(6)	302.10(9)
	1	4.54(9)	4.8358(13)	5.3673(11)	6.0579(15)	99.95(3)	104.284(19)	91.76(2)	149.64(7)	299.27(9)

The equations of state for phases α-γ were refined with EoSFit7c[19] from the volume data in Table S5 using a Birch-Murnaghan model. The refined parameters are reported in Table S6, and were used for plotting the lines in Figure 2 (main text).

Table S6. Refined parameters for the equations of state of phases **1** α-γ.

Phase name	α	β	γ
EoS order	3	3	2
V_0	374.35001	369(3)	338.4(20)
K_0	10.0(6)	11.1(20)	29.0(19)
K_p	15(2)	8.3(17)	4.000
K_{pp}	-13.08804	-2.40843	-0.13404

Structure refinement of γ–[$CuF_2(D_2O)_2$(pyz)]

Ground $CuF_2(D_2O)_2$(d_4-pyz) crystals were loaded into a Merrill-Bassett type DAC equipped with 0.5 mm diamonds and a steel gasket, preindented to 0.084 mm with a 0.2 mm hole. The pressure was quickly raised to 3.8 GPa, as determined from ruby fluorescence[13] and the sample equilibrated for ca. 580 h. Pressure medium consisted of 92% isopropanol with 8% H_2O.

Data were collected at X06DA - PXIII (Macromolecular Crystallography Beamline) at Swiss Light Source, Paul Scherrer Institute, Villigen, Switzerland, equipped with a Dectris Pilatus 2M area detector using 17.5 keV X-radiation. Acquired images were converted with SNBL Toolbox[20] and subsequently integrated with Fit2D.[21] Sample position and detector distance were calibrated from NIST SRM 660a LaB_6 in an unpressurized DAC.

Starting from coordinates of **β-1**,[3] the structure of **γ-1** was simultaneously refined against seven datasets with Topas-Academic.[18] The center of a rigid body model for the pyrazine ring was set to 0.5, 0.5, 0.5 (three rotation parameters) and Cu was set to 0, 0, 0. x, y, z coordinates of F and O were freely refined. The two D sites around oxygen were defined as rigid body with center at the O position (three rotational parameters). B_{iso} values of 1.5 Å^2 for non- and 3 Å^2 for D were not refined. The background was taken from the LaB_6 dataset. Background scale and y-shift, TCHZ profile[22] and lattice parameters were determined from Pawley refinements and kept fixed for subsequent refinement steps. This resulted in a ratio of 13 structural parameters vs. 124 observed peaks in each of the seven patterns. Two regions were excluded (one for the gasket-peak and another one for an unknown artifact in all frames).

Lattice parameters and refinement data, site coordinates, selected geometric parameters and H-bond details of the refined and calculated structures are listed in Tables S7 to S9.

Periodic Density Functional calculations

Periodic B3LYP calculations using full electron 6-31G(d,p) basis set were carried out with CRYSTAL09[7] on all the phases reported in the text, whose geometries were optimized in the range at 0-3.0 GPa. A full description of the structural details and the energy will be reported elsewhere.[10] Here we report data for the the predicted phase **γ-1** and the spin density maps for all the phases, showing the orbital reordering.

Table S7. Lattice parameters and refinement data of **γ-1**.

γ-$CuF_2(H_2O)_2(pyz)$		
Empirical formula, M_r	$C_4D_8CuF_2N_2O_2$	225.71 g mol^{-1}
T, P	298 K,	3.8 GPa
λ	0.70848 Å	
Crystal system	Monoclinic	
Space group, Z	$P2_1/c$,	2
	Refinement	**P-B3LYP Simulation**
Unit cell dimensions*	a = 6.8112(6) Å	a = 6.78340 Å
	b = 7.6632(6) Å	b = 7.83931 Å
	c = 6.5422(8) Å	c = 6.50904 Å
	β = 117.318(10) °	β = 116.88129 °
Volume*	303.39(6) Å^3	308.731 Å^3
d-range	6.06 to 1.35 Å	
Excluded regions	2.52 to 2.39 and 2.10 to 1.96 Å	
Refined parameters	13	
Weighting scheme	$1/\sigma(I_{obs})$	
R_{wp} Rietveld (min./max. of 7 patterns)	1.81/2.16 %	
R_{Bragg} Rietveld (min./max. of 7 patterns)	12.5/13.5 %	
R_{wp} Pawley (min./max. of 7 patterns)	0.55/0.56 %	
R_{Bragg} Pawley (min./max. of 7 patterns)	0.01/0.02 %	

* From Pawley refinements

Table S8. Site coordinates of refined and simulated structures of **γ-1.**

Site	$x_{\text{Refinement}}$	$x_{\text{P-B3LYP}}$	$y_{\text{Refinement}}$	$y_{\text{P-B3LYP}}$	$z_{\text{Refinement}}$	$z_{\text{P-B3LYP}}$
Cu1	0	0	0	0	0	0
F2	0.148(3)	0.0629	0.737(2)	0.7245	0.104(4)	0.0524
O3	0.217(3)	0.1529	1.000(7)	1.0134	0.348(5)	0.3431
D31	0.11(7)	0.0742	1.10(5)	1.1051	0.32(8)	0.3844
D33	0.14(8)	0.1338	0.90(4)	0.9074	0.38(7)	0.4169
N4	0.715(3)	0.7017	0.502(8)	0.5084	0.533(8)	0.4985
C5	0.346(8)	0.3416	0.400(4)	0.3939	0.336(4)	0.3585
D51	0.224(15)	0.2115	0.320(8)	0.3130	0.205(7)	0.2407
C6	0.563(10)	0.5447	0.403(5)	0.4028	0.370(6)	0.3565
D61	0.616(19)	0.5845	0.326(9)	0.3254	0.268(10)	0.2444

Table S9. Selected geometric parameters and H-bond details for **γ-1**.

Sites	Distance (Refinement) /Å	Distance (P-B3LYP) /Å
Cu – F	2.215(16)	2.198
Cu – N	2.054(12)	2.020
Cu – O	2.07(3)	1.995
O – D ··· F	1.8(2)	1.569
O – D ··· F	2.2(2)	1.502

Sites	Angles (Refinement) /°	Angles (P-B3LYP) /°
F – Cu – F	180	180
F – Cu – N	106(2)	95.30
F – Cu – N	74(2)	84.70
F – Cu – O	109.5(15)	95.05
F – Cu – O	70.5(15)	84.95
N – Cu – O	96.7(16)	91.14
N – Cu – O	83.3(16)	88.86
N – Cu – N	180	180
O – Cu – O	180	180

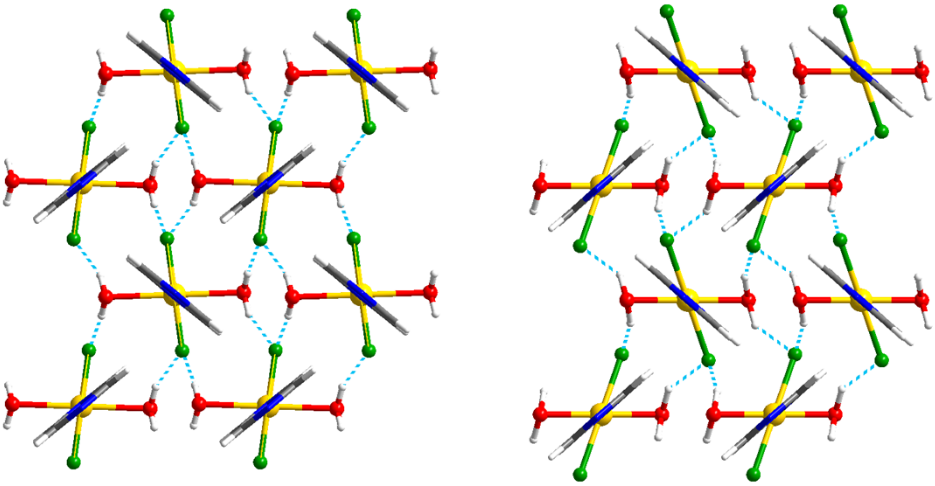

Figure S2 – Comparison of the crystal packing of **β-1** (left) and **γ-1** (right) in the *bc* crystallographic plane.

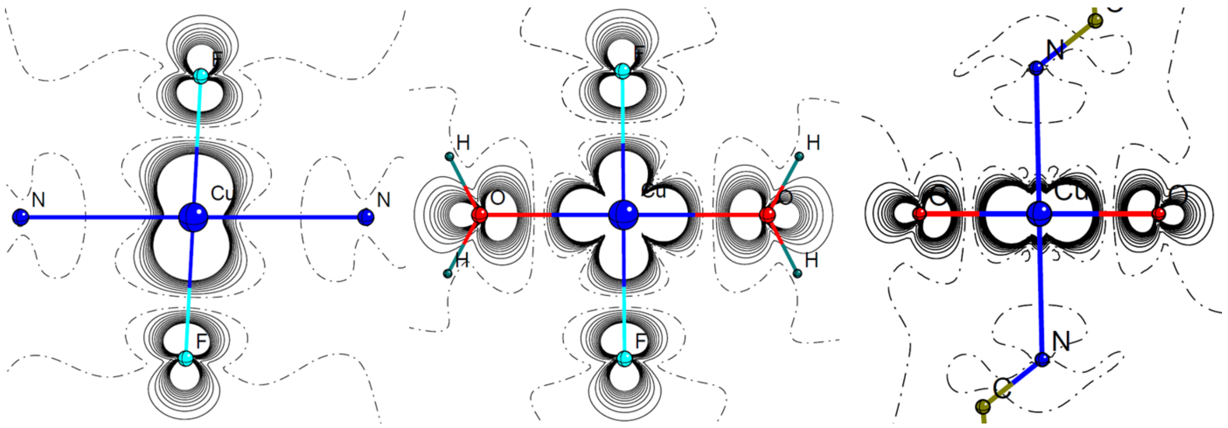

Figure S3 – Spin density maps in **α-1**, calculated at 0.0 GPa: left the plane formed by Cu, N(pyz) and F; center, the plane formed by Cu, F and O(H_2O), right, the plan formed by Cu, O(H_2O) and N(pyz). Solid contours represent positive spin plotted with logarithmic increase; dashed-dot lines are 0.0 spin density.

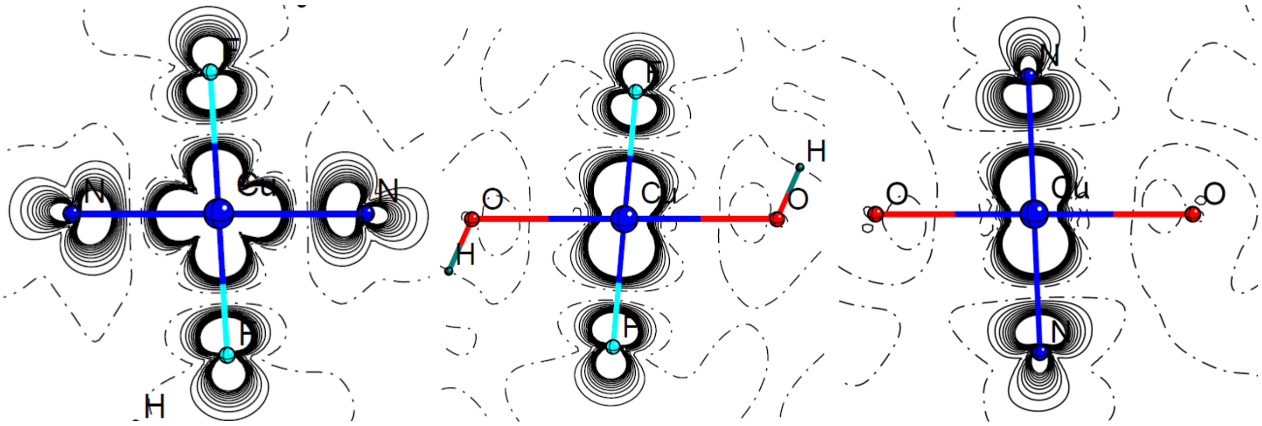

Figure S4 – Spin density maps in **β-1**, calculated at 3.0 GPa: left the plane formed by Cu, N(pyz) and F; center, the plane formed by Cu, F and O(H_2O), right, the plan formed by Cu, O(H_2O) and N(pyz). Solid contours represent positive spin plotted with logarithmic increase; dashed-dot lines are 0.0 spin density.

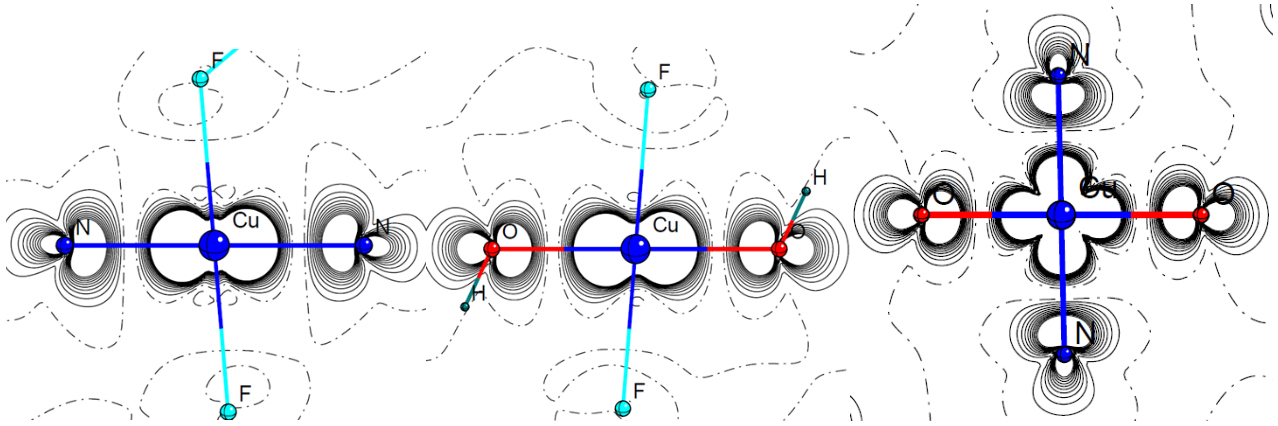

Figure S5 – Spin density maps in **γ-1**, calculated at 3.0 GPa: left the plane formed by Cu, N(pyz) and F; center, the plane formed by Cu, F and O(H_2O), right, the plan formed by Cu, O(H_2O) and N(pyz). Solid contours represent positive spin plotted with logarithmic increase; dashed-dot lines are 0.0 spin density.

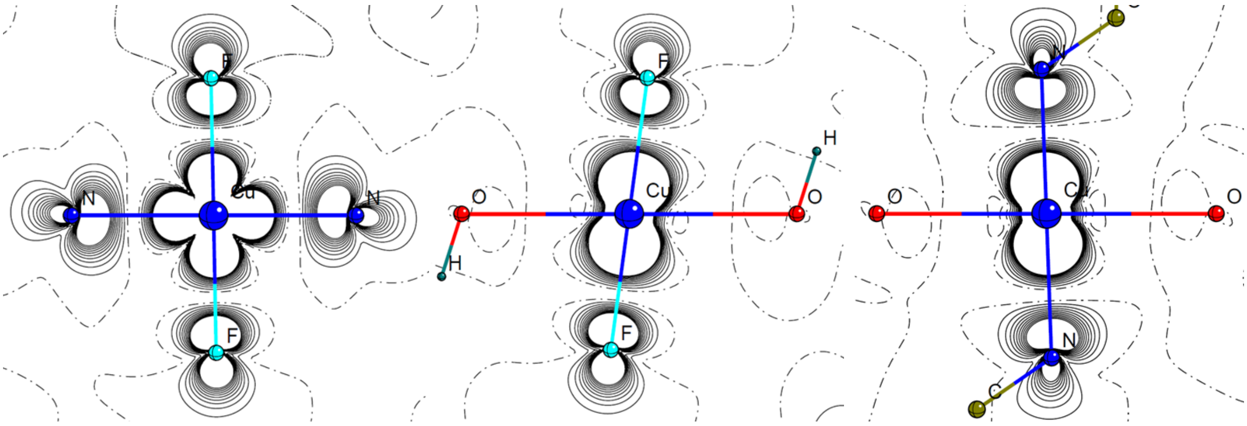

Figure S6 – Spin density maps in **ε-1**, calculated at 3.0 GPa: left the plane formed by Cu, N(pyz) and F; center, the plane formed by Cu, F and O(H_2O), right, the plan formed by Cu, O(H_2O) and N(pyz). Solid contours represent positive spin plotted with logarithmic increase; dashed-dot lines are 0.0 spin density.

Characterization of $[(CuF_2(D_2O)_2)_2(pyz)]$ (2)

SC-XRD

A single crystal of **2** was mounted with glue on a glass needle and the diffracted intensities were collected at 298 K. The crystal did not show decomposition during the data collection time. All measurements were made with an Oxford Diffraction SuperNova area-detector diffractometer using mirror optics monochromated Mo Kα radiation ($\lambda = 0.71073$ Å). A total of 764 frames were collected in 1° ω steps, 5 s exposure time and a fixed sample-detector distance of 66.2 mm; CrysAlisPro[14] was used for the data collection, data reduction and empirical absorption correction. The crystal structure was solved by direct methods with SHELXS-2013[15] and least-squares refined with SHELXL-2013[15] using anisotropic thermal parameters for all non-D atoms. D atoms for the pyrazine ring were assigned geometrically and refined with a riding model with U_{iso} equal to 1.2 times that of the corresponding parent atom. D atoms pertaining to the coordinated water molecule were located in the Fourier difference map. The results of this experiment are reported in Tables S10 and S11.

Table S10. Crystal data and structure refinement for **2** at R.T. and ambient *P*.

$(CuF_2(H_2O)_2)_2(pyz)$	CCDC 998111	
Empirical formula, M_r	$C_2 D_6 Cu F_2 N_2 O_2$	183.65 g mol^{-1}
T, *P*	298(2) K,	10^{-4} GPa
λ	0.71073 Å	
Crystal system	Monoclinic	
Space group, *Z*	*I*2/*c*,	8
Unit cell dimensions	a = 21.0200 (3) Å	α= 90 °
	b = 7.5530 (1) Å	β= 98.456 (2) °
	c = 6.8810 (1) Å	γ = 90 °
Volume	1080.58 (3) Å^3	
Crystal dimensions	1 × 0.23 × 0.17 mm^3	
Density (calculated), μ	2.258 Mg m^{-3},	3.994 mm^{-1}
F(000)	704	
θ range	1.959 to 31.738 °	
Index ranges	-30<=h<=30, -11<=k<=10, -9<=l<=10	
Reflections (unique), R_{int}	6919 (1747),	0.018
Parameters (restraints)	90 (0)	
Goodness-of-fit on F^2	1.100	
R indices [I>2σ(I)]	$R_1 = 0.0191$,	$wR_2 = 0.0583$
R indices (all data)	$R_1 = 0.0265$,	$wR_2 = 0.0654$
Largest diff. peak and hole	0.354 and -0.450 e.Å^{-3}	

Table S11. Selected geometric parameters and H-bonds details for **2**.

atoms[a]	*distance* /Å	*atoms*	*distance* /Å
Cu1—F1	1.8935(10)	Cu1—O2	1.9664(13)
Cu1—F2	1.8987(10)	Cu1—N1	2.4040(16)
Cu1—O1	1.9932(13)	Cu1—O1^{i}	2.5221(13)
atoms	*angle* /°	*atoms*	*angle* /°
F1—Cu1—F2	177.26(4)	O2—Cu1—O1	175.32(5)
F1—Cu1—O2	89.07(4)	F1—Cu1—N1	90.89(4)
F2—Cu1—O2	89.62(4)	F2—Cu1—N1	91.54(4)
F1—Cu1—O1	90.82(4)	O2—Cu1—N1	90.92(6)
F2—Cu1—O1	90.29(4)	O1—Cu1—N1	93.75(6)

X—D···*A*[a]	*X*···*A* /Å	*X*—D···*A* /°[b]
O1—D1*A*···F1^{ii}	2.5996(14)	170(2)
O1—D1*B*···F2^{iii}	2.6177(14)	169(2)
O2—D2*A*···F2^{iv}	2.6046(14)	167(2)
O2—D2*B*···F1^{v}	2.5905(14)	165(2)
C1—D1···F2^{iii}	3.3228(18)	156

[a] Symmetry codes: (i) -*x*, *y*, -*z*+3/2; (ii) *x*, -*y*, *z*-1/2; (iii) *x*, *y*+1/2, *z*-1/2; (iv) *x*, -*y*+1, *z*+1/2; (v) *x*, -*y*, *z*+1/2. [b] The uncertainty is not given in case the H coordinates are not freely refined.

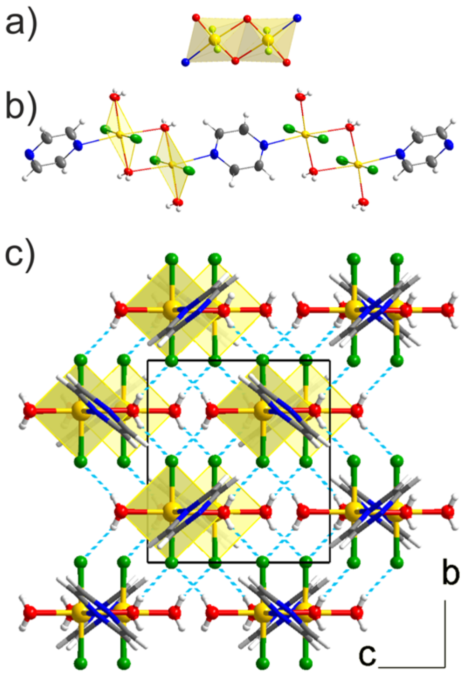

Figure S7 – Views of compound **2**: (a) Edge-sharing Cu coordination octahedra; (b) The magnetic orbitals (highlighted as yellow squares are approximately perpendicular to the direction of the polymeric chains; (c) Crystal packing in the *bc* plane showing the H-bond mediated 2D magnetic exchange pathways.

Magnetic measurements

Ambient pressure magnetic measurements were performed on a Quantum Designs MPMS SQUID-XL magnetometer. Crystals of **2** were quickly dried and ground with a drop of liquid nitrogen. 19.1 mg of a powdered sample of compound **2** and 42.16 mg of **1** were mounted in gelatine capsules. The samples were cooled in zero field and susceptibility experiments were conducted at an applied magnetic field of 250 Oe between 1.9-250 K for **1** and **2**. In addition, compound **2** was measured at fields from 50 Oe up to 2500 Oe. The measurements were corrected for core diamagnetism using Pascal's constants. The signal of the sample holder and capsule was subtracted by using the measurement of a blank capsule at 250 Oe, which was corrected for the mass of the capsules used for the measurements of **1** and **2**. Magnetic susceptibility was simulated with the ALPS package.[23]

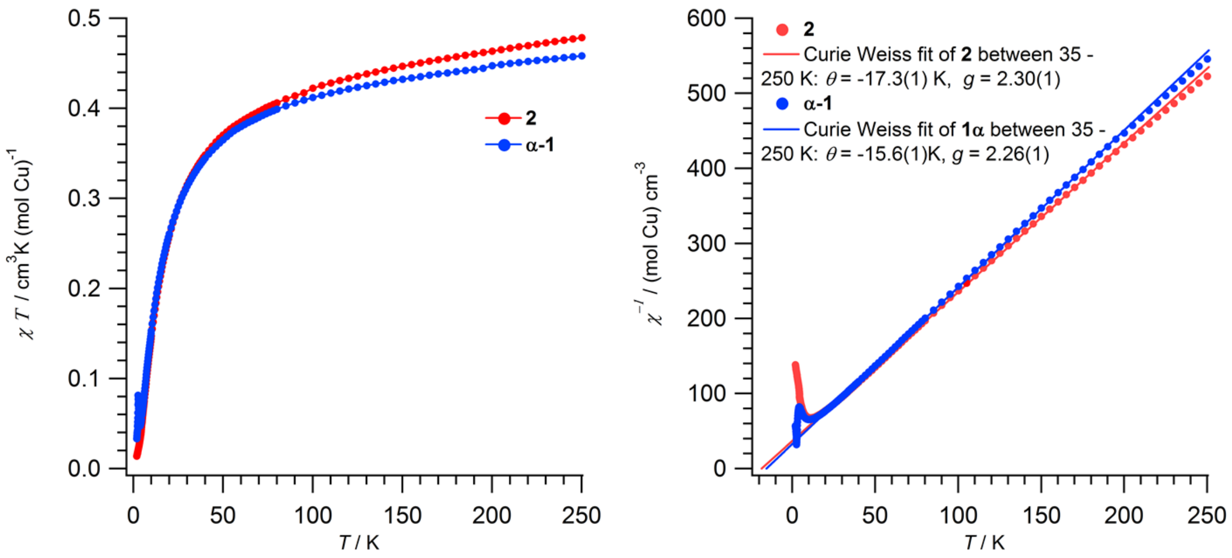

Figure S8 – χT (left) and $1/\chi$ (right) of **α-1** and **2** as a function of T measured at 250 Oe.

Periodic Density Functional calculations

Periodic B3LYP calculations using 6-31G(d,p) basis set were carried out with CRYSTAL09[7] on the crystal structure of **2** at 0.0 GPa. The spin density maps demonstrate the direction of the magnetic orbital.

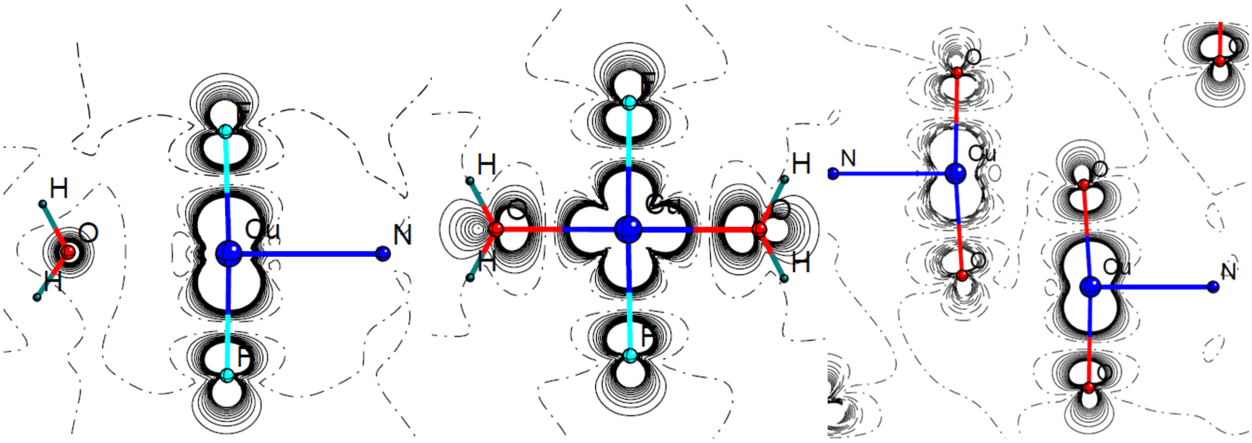

Figure S8 – Spin density maps in **2**, calculated at 0.0 GPa: left the plane formed by Cu, N(pyz,), O(H_2O bridge) and F; center, the plane formed by Cu, F and O(H_2O); right, the plane formed by Cu, N(pyz) and O(H_2O, bridge). Solid lines and dotted lines contours represent positive and negative spin density respectively, plotted with logarithmic increase; dashed-dot lines are 0.0 spin density.

Additional references

[13] K. Syassen, *High Pressure Res.* 2008, **28**, 75-126.

[14] CrysAlisPro, Agilent Technologies, Version 1.171.36.32, (release 02-08-2013 CrysAlis171 .NET).

[15] G. M. Sheldrick, *Acta Crystallogr. Sect. A* 2008, **64**, 112-122.

[16] P. R. Willmott, D. Meister, S. J. Leake, M. Lange, A. Bergamaschi, M. Boege, M. Calvi, C. Cancellieri, N. Casati, A. Cervellino, Q. Chen, C. David, U. Flechsig, F. Gozzo, B. Henrich, S. Jaeggi-Spielmann, B. Jakob, I. Kalichava, P. Karvinen, J. Krempasky, A. Luedeke, R. Luescher, S. Maag, C. Quitmann, M. L. Reinle-Schmitt, T. Schmidt, B. Schmitt, A. Streun, I. Vartiainen, M. Vitins, X. Wang, R. Wullschleger, *Journal of Synchrotron Radiation* 2013, **20**, 667-682.

[17] R. J. Angel, D. R. Allan, R. Miletich, L. W. Finger, *Journal of Applied Crystallography* 1997, **30**, 461-466.

[18] A. Coelho, Topas Academic Version 5, Coelho Software, Brisbane, 2012.

[19] R. J. Angel, M. Alvaro, J. Gonzalez-Platas, *Zeitschrift für Kristallographie* 2014, **229**, 405-419.

[20] V. A. Dyadkin, SNBL Tool Box v. 0.5 Release 2013-1, Swiss Norwegian Beam Lines at ESRF, Grenoble, France.

[21] A. P. Hammersley, S. O. Svensson, M. Hanfland, A. N. Fitch, and D. Häusermann, *High Pressure Research* 1996, **14**, 235-248.

[22] P. Tompson, D. E. Cox, and J. M. Hastings, *Journal of Applied Crystallography* 1987, **20** 79-87.

[23] A. F. Albuquerque, F. Alet, P. Corboz, P. Dayal, A. Feiguin, S. Fuchs, L. Gamper, E. Gull, S. Gürtler, A. Honecker, R. Igarashi, M. Körner, A. Kozhevnikov, A. Läuchli, S. R. Manmana, M. Matsumoto, I. P. McCulloch, F. Michel, R. M. Noack, G. Pawłowski, L. Pollet, T. Pruschke, U. Schollwöck, S. Todo, S. Trebst, M. Troyer, P. Werner, and S. Wessel, *Journal of Magnetism and Magnetic Materials* 2007, **310**, 1187-1193.